



# Multi-term islanding protection and load priority-based optimal shedding framework for maintain voltage stability loadability in microgrid system

Mohan Kuppusamy<sup>1</sup> · N. Muthukumar<sup>2</sup> · R. Raja Lakshmi<sup>3</sup> · Ralli Sangno<sup>4</sup>

Received: 19 June 2023 / Accepted: 18 November 2023 / Published online: 27 December 2023  
© The Author(s), under exclusive licence to Springer-Verlag GmbH Germany, part of Springer Nature 2023

## Abstract

High dependability, efficiency and low carbon emissions are just a few of the many potential environmental advantages of distributed generation (DG), which is used widely. Accurate islanding detection and quick DG disconnection were crucial to avoid safety concerns and equipment damage brought on by the island mode actions of DGs. Several researchers concentrate on island detection and load scheduling separately. The proposed work focused on islanding detection and load shedding during an island condition. A sophisticated, intelligent mode detection controller detected the system circumstance, and an intelligent shedding controlled the optimal load shedding. The proposed model used a standard IEEE 30-bus system with voltage and current parameters sensed by sensors and given inputs to the intelligent mode detection controller. If the island condition was predicted to move on load scheduling or normal condition was predicted, electricity continued to the utility grid and fulfilled the consumer's required power. The load shedding working process includes system design, data collection and the creation of efficient load scheduling. Maintain steady voltage stability margin throughout that time to complete that priority-based shedding depending on the power generation and its accompanying load restriction. The proposed method was tested for two operating modes, namely detection of islanding modes and load shedding. The proposed approach provides better results in both modes and maintains voltage stability across the entire time period. The proposed method offered a better accuracy of 99% for islanding detection mode when the results were contrasted with those from several other existing methods to validate the performance. As a result, it can be demonstrated that the suggested approach offers better islanding detection performance as well as load shedding with a constant voltage stability margin.

**Keywords** Islanding detection · Real dataset generation · Optimal load shedding · Standard bus system · Voltage stability margin

## 1 Introduction

Even with a significant growth in transmission and distribution, the amount of electricity available still cannot keep up with the demand. A feasible solution in this situation would appear to be distributed generation (DG) based on renewable energy supplies. They can, however, be combined with fuel cells and other storage devices to form a hybrid system for dependable and increased power quality (PQ) because wind speed and solar irradiation intensity are erratic [1]. However, given the wide penetration of these systems, there are significant concerns with islanding occurrence events and PQ issues that need to be addressed. After the occurrence of islands, it is standard practice to immediately disconnect all DRs. The main issues with such island systems are as follows: (1) The voltage and frequency supplied to customers in

---

✉ Mohan Kuppusamy  
kmohangecebargur@gmail.com

<sup>1</sup> Department of Electrical and Electronics Engineering, Government College of Engineering, Bargur, Krishnagiri 635104, Tamil Nadu, India

<sup>2</sup> Centre for Computational Imaging and Machine Vision, Department of ECE, Sri Eshwar College of Engineering, Coimbatore 641202, Tamil Nadu, India

<sup>3</sup> Department of ECE, Panimalar Engineering College, Poonamallee, Chennai 600123, Tamil Nadu, India

<sup>4</sup> Department of EEE, NIT Arunachal Pradesh, Jote 791123, Arunachal Pradesh, India

the islanded system may vary significantly if the distributed resources in the island do not provide regulation of voltage and frequency; (2) islanding may put utility workers in danger by maintaining an energized line; (3) the distributed resources in the island may be damaged when the island is out-of-phase reconnected to the EPS; and (4) islanding may harm the system's distributed resources [2].

The most popular islanding detection techniques can be categorized using remote and local tactics. Complete interaction between the DGs and the utility grid control centre is required for global or remote approaches. Local techniques can also be divided into three types, such as passive, active and hybrid techniques, and artificial intelligence (AI)-based. Passive methods measured the parameters including voltage, frequency, active power, reactive power phase angle, impedance and harmonic distortion to detect the island condition. Active method varies the reactive power to help destabilize the island and accelerate the dissolving of the system to extinguish the island. Same as the hybrid model works based on monitoring the voltage unbalance and changing frequency set point of the DG. AI-based approaches are more effective than these models because it takes a number of inputs to provide an effective outcome. These methods examine the network parameters at the point of common coupling (PCC), which connects the DG site to the utility network, including voltage, current, frequency and harmonic distortion, in order to find instances of islanding [3]. The signal is measured and analysed at the terminal of distributed energy resources (DER) or PCC in the active type when a small disturbance has been injected into the electrical networks. The injected disturbance, however, significantly affects the network parameters when islanding occurs [4]. To precisely define the islanding condition, several methods have been devised. The most cost-efficient and efficient method is to combine a passive methodology with artificial intelligence [5], because it has been successfully used to accurately monitor electricity systems online [6]. Some methods developed for detecting island conditions were hybrid islanding detection mechanism (IDM) [7], power conversion system (PCS) [8], long short-term memory (LSTM) [6, 9], local synchrophasor measurements [10] and direct current microgrid (DC-MG) [11]. However, in case of specific type of non-islanding event such as triple-line fault on adjacent feeder, these methods do not give satisfactory results. Also, there are many less performance, high cost and reliability issues. Hence, it is necessary to develop a more efficient signal processing method for islanding detection and classification [12].

The idea of promptly disconnecting all DGs is no longer applicable given the recent advancement of new technologies in order to prevent equipment damage and reduce safety threats [13]. The technological challenges in ensuring the secure and efficient operation of islanded events are the speed

governor response, operational power range, voltage and frequency regulation, earthing or a similar type of protection for the operation of the island, and resynchronization to the grid [14]. Voltage and frequency control problems tend to be the most common of these technical problems, and load shedding is thought to be the most successful solution [15]. To restore the voltage and frequency of an islanded system to their nominal values, a load shedding technique must be utilized to reject a number of loads [16]. Researchers have proposed various types of load shedding strategies, with the most practical one being optimal load scheduling employing computational techniques, like adaptive neuro-fuzzy inference system [17], artificial neural network (ANN) [18], fuzzy logic control [19], particle swarm optimization and genetic algorithm [20]. Those models have the ability to learn by themselves and produce the output that is not limited to the input provided to them. But some of the drawbacks are less reliable, high cost and less performance. So a novel intelligent island detection and load scheduling system is developed to detect the islanding condition and schedule the load at the island period to fulfil the load requirements. This proposed model is effective to operate, reduces consumer cost and has high reliability and performance. The main contribution of the proposed model was discussed as follows:

- An intelligent detection system is designed to identify the island/fault condition in an IEEE 30-bus system. In the occurrence of an islanding circumstance, move to a priority-based optimal load shedding model.
- A standard IEEE 30-bus system is designed, in that G1 is assumed as utility grid, and the remaining generator is assumed as a renewable energy resource.
- A real-time dataset is designed which contains the power value of each generator bus during normal and various fault/islanding conditions.
- A novel island detection controller is designed based on the generated dataset to detect the system's condition like normal or fault/island.
- In island conditions, power shortage occurs; to overcome these issues, priority-based load scheduling model is done by using Aquila optimization (AO).
- Generating power, load demand and islanding power are initialized to shed the load during the particular fault period. The best shed is identified by maximizing the VSM and remaining load, which is taken as the objective function of the AO.

The remaining part of the manuscript is structured as the related work of the suggested model is presented in Sect. 2. The general design and procedure of the suggested method are discussed in Sect. 3. The performance validation of the suggested model is given in Sect. 4. Section 5 provides the work's overall conclusions.

## 2 Related work

One of the biggest challenges faced by today's power system is the quick and precise identification of islanding and load scheduling. Numerous models were designed to detect the islanding condition and load scheduling in a microgrid. A few of them are discussed below.

### 2.1 Islanding detection

In this section, only the islanding detection models are reviewed. Islanding conditions are caused due to external disturbance. It is necessary to detect the island condition because the effect of the islanding condition is more dangerous for utility workers. Some of the islanding detection models are discussed as follows.

Elshrief et al. [21] presented a phenomenon as fast and accurately as possible using the technique of rate of change of power based on the terminal voltage of the photovoltaic inverter. This detection method is based on the real power imbalance, which causes transients in an islanded system. When that happens, the system's frequency drifts up or down, making the system's frequency deviate from its nominal value according to IEEE and IEC standards. This model employed a technique based on the PV inverter to quickly and accurately detect the occurrence. However, there is a lack of an appropriate origination to use a hybrid technique that incorporates local and smart techniques such as adaptive fuzzy.

Abdelsalam et al. [22] developed a model for identifying islanding conditions in an MG. This method consisted of two parts, the first of which involved extracting some features from the voltage and current signals and then analysing them to determine the second harmonic using the discrete Fourier transform (DFT). Different case studies are conducted in order to verify the performance of the proposed methodology in detecting the occurrence of islanding and in distinguishing between islanding events and non-islanding events. But LSTMs were over prone to overfitting, and applying the dropout algorithm to curb this issue was difficult.

Karimi et al. [23] developed a method utilizing local synchro phasor measurements as a passive islanding forecasting method in MG, making use of the voltage and current phasors that were recorded at the DG connection point. This method involved using microphasor measuring equipment to keep track of the voltage-to-current ratio and the rate at which the voltage and current magnitudes changed at the PCC. The proposed method has 99.8% accuracy, 99.89% security, 98.11% reliability, zero non-detection zone and detection time of 49 ms. The simulation demonstrated that the scheme was reliable, quick, accurate and easy to use for inverter-based DGs. Compared to the hybrid technique, the passive technique was not much good.

Dutta et al. [24] suggested an island detection method was developed, which used both the software and hardware modules of microphasor measurement unit ( $\mu$ PMU). The method involves detecting the voltage signals of specified solar generator buses using a PMU and then using spectral kurtosis (SK) to extract hidden signal information needed to feed a random forest (RF) classifier for distinguishing inability and island situations from other cases. The results were also communicated to other solar generator (SG) in the region through communication channels. The method was poor to perform at continuous fault periods.

Ali et al. [25] developed a simple Internet of Things (IoT)-based protocol that was used to convey the voltage and frequency of each DG through an edge device (ED). Context-aware policy (CAP) was put into place in ED to enhance traffic flow across a communication network (CN) by comparing the current and prior data values. A cloud-based machine learning (ML) model for ANN islanding detection was developed in the third layer. Data generated through islanding mode was used to train the model. A centralized cloud-based real-time islanding detection scheme was applied using ANN by sending PMU data through an IoT network. The cloud received PMU data for island prediction. However, the model designing was much more complex and high cost.

Ramachandradurai et al. [26] suggested a modified passive islanding detection strategy that coordinates the V–F (voltage–frequency) index was developed to reduce the non-detection zones (NDZs). The power mismatch was alleviated in the identified islands by installing a battery and a diesel generator, which prevented islanding events. The method uses here is a passive method in which an islanded bus is identified in the presence of DG units in a distribution system with different ratings.

The above-mentioned related work contains islanding detection; however, the models have common drawbacks like more complex and high cost [22], poor to perform at continuous fault periods [21], not much good to process [24] and lack of an appropriate origination [23]. An advanced technique is created to address these problems, enhancing the system's high reliability and low cost for load scheduling and island detection.

### 2.2 Load scheduling

In a microgrid, load scheduling is crucial for lowering costs and managing consumer power flows depending on priority. Traditional load scheduling methods relied on numerical analysis, but with recent technological advancements, artificial intelligence has been frequently applied. Some of the related work for scheduling the load is discussed below.

Alhelou [27] developed an effective priority-based load shedding strategy for an AC/DC microgrid (MG) using

micro-PMU data. In this study, a priority-based load is developed. The location and intensity of load shedding are determined using a flow tracing technique for power-consuming AC/DC microgrids. By considering the importance of the loads on the islanded in substantial network outages, a microgrid can use this strategy to ensure the power for important loads. However, the model's performance is not very good. Rauf, et al. [28] developed a priority-based paradigm to manage and run rural DC-MGs. The supervisory control and data acquisition (SCADA) system has been integrated to evaluate the priority-based algorithms in a laboratory setting. The approach focuses primarily on creating a suitable method for supplying dependable power to the rural areas of emerging nations. However, this system requires more time to complete a process.

Hassan et al. [29] presented a load shedding (LS) technique based on priority demands (PDs) considering the wind power generation. This strategy allows us to prioritize the loads based on their importance and apply logarithmic RM while considering the penetration and the wind power. The simulation findings revealed decreased demands while providing energy to the crucial loads that were kept operating. The system's dependability and efficiency were increased via selected LS for the essential loads. However, the system's dependability is low. Mogaka et al. [30] presented priority indices for loads linked to the various buses are determined using the Fast Voltage Stability Index. The amount of load that must be shed is then assessed using the artificial bee colony (ABC) algorithm to ensure that the linked loads and power generated within an island microgrid are balanced. However, it is difficult to forecast the load demand at the fault period.

Awad et al. [31] suggested operating the under-frequency load shedding (UFLS) relays as efficiently as possible, providing a reliable multi-objective hybrid optimization algorithm that combines PSO and BF (HPSBF) method. The convergence rate and the superiority of the identified solution are two benefits that the optimizer incorporates from particle swarm (PSO) and bacterial foraging (BF). The IEEE 9-bus and IEEE 39-bus standard systems are used to examine the acceptability and feasibility of the HPSBF under various disturbances, such as a single plant failure, simultaneous outages of several plants and a significant increase in linked loads. However, the model's performance is inadequate.

Sarasúa et al. [32] suggested an alternative control strategies in one of the Canary Islands (El Hierro Island) in terms of reducing the need of load shedding activation. These control strategies are the variable speed wind turbines inertial contribution to frequency regulation and the use of Pelton turbines as synchronous condensers. The participation of variable speed pumps in the frequency regulation, control strategy recently adopted in El Hierro power system, has been included in the analysis. Xu et al. [33] developed a

phase measurement unit (PMU)-based online load shedding strategy and a conservation voltage reduction (CVR)-based multi-period restoration strategy that are proposed for the intentional island with renewable distributed generation. When the blackout occurs, the correction table updated in real time based on the PMU data is used to modify the load shedding plan to eliminate the power mismatch caused by the fluctuation of renewable distributed generation. However, the estimation performance in the transient process is poor since PMU relies on the static signal model, which may result in a wrong load shedding.

The above-mentioned related work contains islanding detection and priority-based load scheduling alone. However, the models have common drawbacks like difficulty in operating, less reliability [30], high cost [31], time consumption [31], planning and load scheduling problems [27] and cannot provide a sufficient outcome [28]. An advanced technique is created to address these problems, enhancing the system's high reliability and low cost for load scheduling and island detection.

### 3 Proposed methodology for islanding detection and load scheduling

Due to the growing use of DGs, the MG is one of the energy supply technologies that have attracted much attention. The control, operating, safety and protection tactics used in grid-connected mode and island mode would differ. Thus, it is crucial to put in place a reliable system to detect accidental islanding conditions in MGs. Once the islanding mode has been detected, the load, which is challenging to manage, is required to meet the load demand. In the proposed model, two phases are introduced to manage the power quality in a system. In phase 1, an intelligent controller is designed to detect whether the system is in islanding mode or normal condition in a standard bus system. Island mode includes short-circuit faults, namely triple-line-to-ground fault (LLLG), double-line-to-ground fault (LLG), load switching, capacitance switching and line-to-ground fault (LG). If the system is normal, there is no need for any scheduling process. If the system is in islanding mode, it cannot handle the full load demand. Therefore, a cutting-edge optimization technique is created to control load shedding during the appropriate island period. Figure 1 shows a process of the suggested model's overall architecture.

The suggested model's architecture consists of two phases, including load scheduling during islanding conditions and the identification of island mode. The first step of the IEEE 30-bus system model studies island detection or grid linked mode. The suggested model comprises six generators, twenty-one loads and 41 transmission lines. Sensors measure the voltage and current parameters. The recurrent

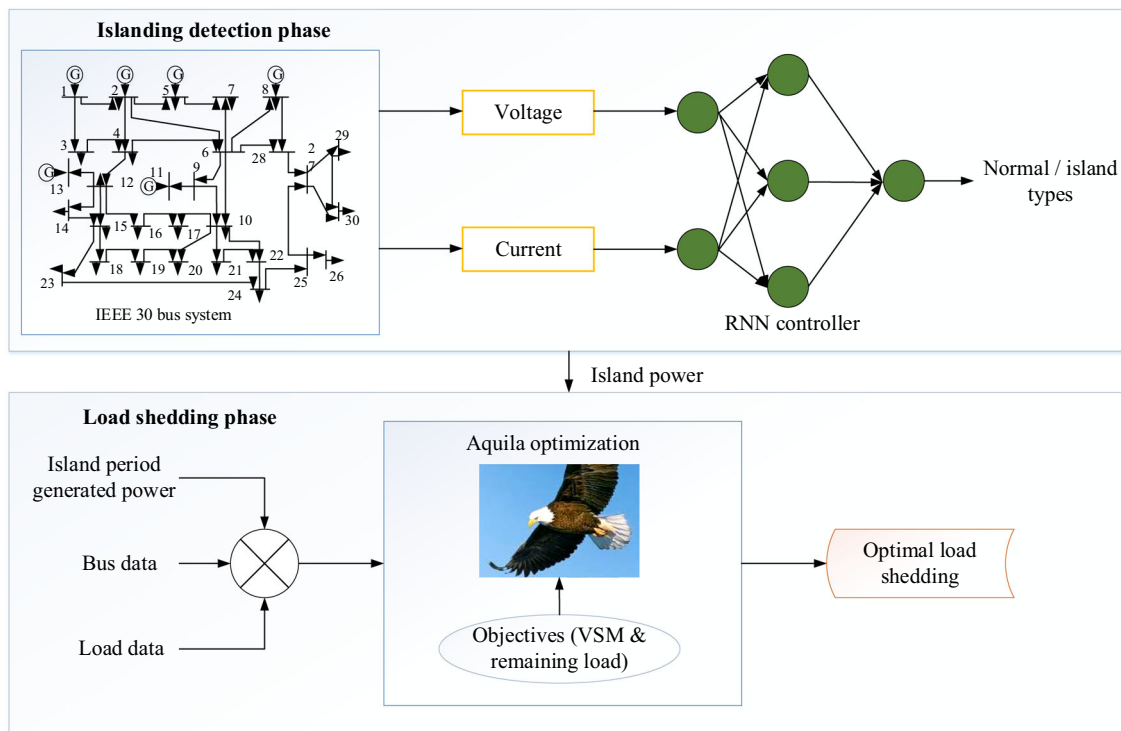


Fig. 1 Architecture of proposed model

neural network (RNN) controller provides the voltage and currents. Multiple datasets can be handled by RNNs, which accept current and historical input data. Due to their internal memory, RNNs can also be trained using historical input. RNN can check the proposed network whether it is island or normal. Island mode includes short-circuit faults, namely triple-line-to-ground fault (LLLG), load switching, double-line-to-ground fault (LLG), capacitance switching and line-to-ground fault (LG). If the islanding condition is detected, proceed with the load scheduling process, or the normal condition occurs power supply continues to the grid. According to the priority of the load, load shedding is carried out. Three categories, such as critical, semi-vital and non-vital, are used to group the loads. First to be shed will be the non-vital load, then the semi-vital and finally the critical load. To increase efficiency during the islanding period, an optimum load shedding approach employs the Aquila optimization (AO) algorithm. In load shedding, initialize the generation, bus data and load data, and then, analyse hourly load demand and generation of the standard bus system. Based on the generation at islanding condition, an optimal load curtailment is done and maintaining constant VSM to shed the load based on its priority. The proposed model sheds the load at six islanding conditions and continuously maintains the VSM.

### 3.1 Modelling of the standard bus system

Microgrid is considered for the IEEE 30-bus system in the proposed model. The network considered in this work is a simplified approximation of the American Electric Power system using the IEEE 30-bus test case. Six generator buses, twenty-one load buses and forty-one transmission lines make up the IEEE 30-bus system. In this proposed model, G1 is assumed as the utility grid remaining generators are assumed as DG and RES.

#### 3.1.1 Modelling of the utility grid

The connection between various levels of voltage is accomplished through a transmission line and all of the transformers. Thevenin equivalent circuit data with ( $Z = R + jX$ ) impedance is used to build the grid system.

$$P_{\text{utility}} = \Delta V / I \tag{1}$$

where  $I$  represent current and  $\Delta V$  denotes potential difference. A realistic method to combine scattered energy resources, increase the reliability of the power supply and reduce operating expenses is provided by the IEEE 30-bus system. Both grid-connected and islanding modes of operation are available for the bus system. In islanding mode, the utility load disconnects the network, whereas grid connector

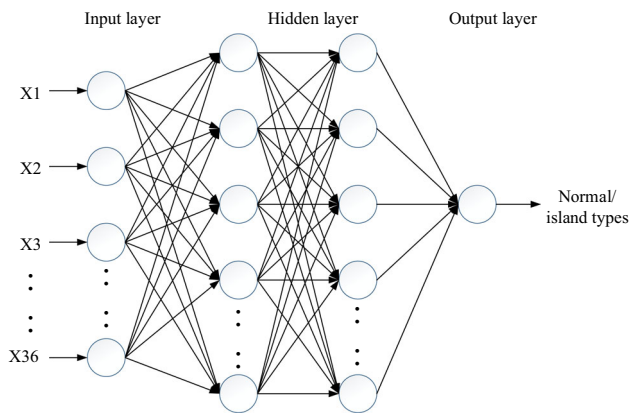


Fig. 2 Recurrent neural network model

mode links utility grids to satisfy load demand. Voltage and current are sensed by using sensors concerning time in island mode or normal power flow to detect whether the system is in normal or islanded condition [34]. If the island is detected, it must shed the load to manage the power flows.

### 3.2 Modelling of intelligent mode detection controller

A neural network is a collection of interconnected layers replicating the human brain's organization and function. It learns from vast amounts of data while employing intricate algorithms to train a neural network. RNN functions under the assumption that each layer's output is saved and fed back into the input to predict that layer's output. The nodes in the different neural network layers are compressed to form a single layer of recurrent neural networks. RNN can manage sequential data, accepting both the data being entered at the present and earlier inputs. RNNs have internal memories that allow them to remember prior inputs. The neural network's input layer gathers and analyses the data before sending it to the intermediate layer. The intermediate layer might contain a number of hidden layers, each with its own bias, weights and activation mechanisms.

In the suggested model, recurrent neural networks can be utilized to create a neural network without memory in which the various hidden layer parameters are independent of one another. To guarantee that the parameters for each hidden layer are the same, the RNN will standardize the various activation functions, weights and biases. Then, rather than using several hidden layers, it will create a single hidden layer and loop over it repeatedly. The suggested model, RNN island detection controller architecture, is illustrated in Fig. 2.

The proposed modelling consists of an IEEE 30-bus system. Each bus has a separate voltage and current sensed by a sensor to generate a dataset. This dataset is given an input of RNN.  $y^t$  and  $x^t$  are the output and input variable step  $t$ .

Based on input  $x^t$  and the preceding hidden state  $s^{t-1}$ , the RNN hidden state  $s^t$  is determined. At step  $t$ , the RNN's input and output variables are  $x^t$  and  $y^t$ , respectively.

$$s^t = f\left((Ux^t + b) + Ws^{t-1}\right) \quad (2)$$

$$o^t = Vs^t + c \quad (3)$$

$$y^t = g(o^t) \quad (4)$$

where  $f = \tanh$  denotes the memory of RNN,  $s^t$  is the hidden layer at step  $t$ ,  $g$  represents the sigmoid activation function of the output layer and the hidden layer,  $W$  is the weight matrix between the hidden layer and hidden layer,  $U$  is the weight matrix between the input layer and hidden layer and  $V$  is the weight matrix between the hidden layer and output layer;  $U$ ,  $V$  and  $W$  are not changed in the different steps. The hidden state is a temporary factor  $o^t$  that determines the parameters  $b$  and  $c$ , which are bias vectors.

### 3.3 Backpropagation algorithm for RNN training

Backpropagation through time, or BPTT, is a recurrent neural network methodology that applies the backpropagation training method to sequence data like a time series. Each time step, one input is presented to a recurrent neural network, which then forecasts the output. Conceptually, BPTT operates by unrolling each input time step. The gradient of the  $b$ ,  $V$ ,  $W$ ,  $U$  and  $c$  parameters is calculated using the backpropagation over time method. A backpropagation training approach for RNNs, or BPTT, trains these networks using sequence data, such as time series.

$$L = \sum_{t=1}^{\tau} \left( \frac{1}{2} (\hat{y}_j^t - y_j^t)^2 \right) \quad (5)$$

where  $L$  represents the time sequences cost function, according to Eq. (5) the sub-costs at each time step add to the final cost. The measured value is  $\hat{y}_j^t$  and the anticipated value is  $y_j^t$ , respectively. The definition of the step  $t$  hidden state gradient is,

$$\delta^t = \frac{\partial L}{\partial s^t} \quad (6)$$

where sub-cost at each subsequent time step  $t + 1$  and  $\delta^t$  depends on both the sub-cost at the current step  $t$ . Therefore,  $t$  is connected to the hidden layer state  $s^{t+1}$  and the output temporary variable  $o^t$

$$\begin{aligned} \delta^t &= \frac{\partial L^t}{\partial o^t} \frac{\partial o^t}{\partial s^t} + \frac{\partial L^{t+1}}{\partial s^{t+1}} \frac{\partial s^{t+1}}{\partial s^t} \\ &= V^T (\hat{y}^t - y^t) g'(o^t) + W^T \delta^{t+1} \text{diag} \left( 1 - (s^{t+1})^2 \right) \end{aligned} \tag{7}$$

where  $\text{diag}(\cdot)$  stands for converting a vector into a diagonal matrix. But there is no more hidden state afterwards step  $\tau$ , and the  $\delta^t$  is expressed as

$$\delta^\tau = \frac{\partial L}{\partial o^\tau} \frac{\partial o^\tau}{\partial s^\tau} = V^T (\hat{y}^\tau - y^\tau) g'(o^\tau) \tag{8}$$

BP is utilized to gradually regulate the gradient of the network parameters at step  $t$ . The gradient of the following variables  $b, c, V, W$  and  $U$  can be represented using the following formula,

$$\frac{\partial L}{\partial c} = \sum_{t=1}^{\tau} (\hat{y}^t - y^t) g'(o^t) \tag{9}$$

$$\frac{\partial L}{\partial V} = \sum_{t=1}^{\tau} \frac{\partial L^t}{\partial o^t} \frac{\partial o^t}{\partial V} = \sum_{t=1}^{\tau} (\hat{y}^t - y^t) g'(o^t) (s^t)^T \tag{10}$$

$$\frac{\partial L}{\partial b} = \sum_{t=1}^{\tau} \frac{\partial L}{\partial s^t} \frac{\partial s^t}{\partial b} = \sum_{t=1}^{\tau} \text{diag}(1 - (s^t)^2) \delta^t \tag{11}$$

$$\frac{\partial L}{\partial W} = \sum_{t=1}^{\tau} \frac{\partial L}{\partial s^t} \frac{\partial s^t}{\partial W} = \sum_{t=1}^{\tau} \text{diag}(1 - (s^t)^2) \delta^t (s^{t-1})^T \tag{12}$$

$$\frac{\partial L}{\partial U} = \sum_{t=1}^{\tau} \frac{\partial L}{\partial s^t} \frac{\partial s^t}{\partial U} = \sum_{t=1}^{\tau} \text{diag}(1 - (s^t)^2) \delta^t (x^t)^T \tag{13}$$

The final gradients of the network parameters are explicitly formed by the sum of the sub-gradients at each time step. Equations (9), (10), (11), (12) and (13) provide a simple to determine the gradients of the network parameters. As a result, the following is the modified rule for these parameters,

$$b^{n+1} = b^n - \eta \frac{\partial L}{\partial b} \tag{14}$$

$$c^{n+1} = c^n - \eta \frac{\partial L}{\partial c} \tag{15}$$

$$V^{n+1} = V^n - \eta \frac{\partial L}{\partial V} \tag{16}$$

$$W^{n+1} = W^n - \eta \frac{\partial L}{\partial W} \tag{17}$$

$$U^{n+1} = U^n - \eta \frac{\partial L}{\partial U} \tag{18}$$

where  $\eta$  represents the number of times the BPTT iteration occurred and is the RNN’s learning rate. The cost function’s partial derivatives with respect to the disturbance of  $b, c, V, W$  and  $U$  can be found using Eqs. (14)–(18). Based on the RNN detection, the next level of the process is decided. That is, if the RNN detects the system condition is in grid-connected mode, there are no changes for power flowing; on the other hand, if the RNN detects the system is in island mode, which includes short-circuit faults such as triple-line-to-ground fault (LLLG), double-line-to-ground fault (LLG), load switching, line-to-ground fault (LG) and capacitance switching, the load must be scheduled for managing load demand. Due to scheduling, the consumer receives the required amount of power without any fluctuation or power cuts. The load shedding model of the islanding mode is discussed in the following section.

### 3.3.1 Load shedding

The most promising demand-side management strategy is load shedding, in which consumers move load from peak to off-peak hours in order to reduce grid power peak and economic loss. In island conditions, occurs leads to load unbalancing. To minimize load unbalancing issues using, load shedding is one of the best ways. This system is made to determine the island’s power imbalance, choose the minimal load to shed and make sure that as many loads as possible are still connected to the system [35]. A vital part of load shedding is load control and management. The primary goals of load shedding in an island situation are maintaining VSM, supplying electricity to associated loads and minimizing losses.

**Design of optimum load shedding** The islanded system’s ideal load shedding is designed to improve the VSM profile. However, it is also essential to consider the following limits while optimizing.

**Problem formulation** The VSM and voltage profile are intended to be improved by the islanded system’s optimal load shedding. However, when optimizing, the following constraints should be taken into account. It is modelled after a typical distribution system’s radial feeder, and branch  $I$  is linked to buses  $k$  and  $m$ . Branch  $I$  loading index ( $L_i$ ) can be defined as follows by considering the size and angle of bus voltages.

$$L_i = \left( 2 \frac{V_m}{V_k} \cos \delta_{km} \right)^2 \tag{19}$$

where  $V_k$  represents the voltage at bus  $k$ ,  $V_m$  represents the voltage at the bus and  $\delta_{km}$  represents the angle between buses  $m$  and  $k$ .

**Voltage stability margin** The best load shedding strategy uses VSM as an indicator to determine how close the system is to voltage breakdown. The maximum load level for a particular segment is approximated by the  $L_i$  index, which is shown in Eq. (19). All feeder branches loading indices have been presumed to be the result of VSM that is expressed below,

$$VSM_{sys} = \prod_{i \in \Omega} L_i \quad (20)$$

where  $\Omega$  denotes the feeder branch set. As a result, the total VSM system made up of numerous feeders can be assessed as,

$$VSM_{sys} = (VSM_1, VSM_2, VSM_3, \dots, VSM_k) \quad (21)$$

where  $k$  denotes the number of feeders. To lower the load on feeders and raise  $VSM_{sys}$  to a suitable level, some loads in the system should be reduced. Using a suitable optimization algorithm, the optimal amount of load that should be removed from the system can be found.

**Power flow balance** As stated in the following equation, the overall power generated at optimization was equalized to the overall power used.

$$\begin{aligned} \sum P_{gi} - \sum P_{di} - \sum P_{loss} &= 0 \\ \sum Q_{gi} - \sum Q_{di} - \sum Q_{loss} &= 0 \end{aligned} \quad (22)$$

where active and reactive powers produced by the system are denoted by  $P_{gi}$  and  $Q_{gi}$ , respectively, whereas active and reactive powers absorbed by the load are denoted by  $P_{di}$  and  $Q_{di}$ . The reactive and active power losses in a system are denoted by the variables  $P_{loss}$  and  $Q_{loss}$ , respectively.

**Voltage stability in bus** To overcome the system's voltage unstable issues, at each bus  $i$  voltage should be kept within its normal voltage  $V_i$ , which is indicated as  $[V_{i-min}, V_{i-max}]$ , where  $V_{i-min}$  is the  $i$ th bus voltage that is allowed to be as low as possible and  $V_{i-max}$  is the highest voltage that is allowed to be as high as possible. The inequality function can be used to express these limits as

$$V_{i-min} \leq V_i \leq V_{i-max} \quad (23)$$

### 3.3.2 Constraints

The following constraints, such as power flow limit, load shed limits and power generator limits, satisfactorily address the projected optimization equality and inequality constraints issue.

**VSM limit** The  $VSM_{sys}$  must be maintained at a specified level in order to maintain the voltage profile within the nominal value. The following is a representation of the  $VSM_{sys}$  limit,

$$0 \leq VSM_{sys} \leq 1$$

Consequently, the  $VSM_{sys}$  can be expressed as,

$$VSM_{sys} \leq 1 \quad (24)$$

**Power flow limit** The maximum thermal limit  $S_{l-max}$  shall not be exceeded in a steady-state operation, while the apparent power  $S_l$  is interconnected by branch  $l$ .

$$S_l \leq S_{l-max} \quad (25)$$

**Load shed limit** The maximum load that can be reduced inside the system is determined by the load priority limit. The absolute minimum load must be maintained for each load to be kept on a priority list. At all times, the ideal load shedding plan should be implemented. Prior to load shedding, bus  $i$  was carrying  $S_l$ , and the priority load limit is  $S_{priority}$ . The potential value for a balanced load demand is  $S_{l-i}$ . The inequality function allows us to express the constraints as follows:

$$S_{priority} \leq S_{l-i} \leq S_l \quad (26)$$

**Power generator limit** To offer the required power for an islanded mode during load shedding, the generator power  $P_{gen}$  must be kept at its highest level.

$$P_{gen} = P_{max} \quad (27)$$

The Aquila optimization is utilized to identify an ideal load shedding strategy at an islanded distribution system. The optimizer identifies the best values after satisfying the constraints and objective functions. The overview of the Aquila optimization (AO) algorithm is stated as follows.

### 3.3.3 Background of AO

Aquila is the most popular birds globally because its hunting courage is more effective. Male Aquila searches lonely, so grabs more prey. Aquila hunts squirrel, rabbits and other animals using their sharpness and velocity. Aquila has also been pointed out as intimidating to full-grown deer. The next important animal in Aquila's food is a squirrel. Aquila follows four processes with different distinct are used that are expressed below,



- The first hunting process is high fly with an upright stoop used for flight birds' hunting. Once Aquila finds prey, it enters with long, low-angle gliding wings—increasing wings. Aquila needs the elevation feature to hunt its successful prey. To act like thunder, the tail and wings are opened shortly before the engagement, and the legs are pushed forward to catch prey.
- The second technique, contour flight by way of a brief glide attack, is thought to be Aquila's most frequently used method. In this technique, the Aquila rises from land at a low level. Hunting for prey involves being cautious, whether the animal is flying or running. For hunting and breeding grouse, ground squirrels or seabirds, this strategy is ideal.
- The third plundering process is the lower plane, which strikes slowly downwards. The Aquila selects its prey and presses against its neck and back in an attempt to enter. This technique is frequently used for low prey species such as hedgehogs, foxes, rattlesnakes, turtles and any animal that lacks an escape reaction.
- The fourth method involves Aquila travelling on the surface and attempting to spasm its prey, to remove young big prey animals from the exposure area by using this approach.

By using this optimization, the best optimal load shed is done at the corresponding island model. The following steps define how to implement the proposed optimal load shedding scheme:

### 3.4 Aquila optimizer-based load shedding

#### 3.4.1 Step 1: initialization

AO is a multi-centre system; the level of evaluation begins with the inhabitants of Aquila's outputs ( $X$ ) randomly generated between the lower band (LB) and the upper band (UB) of the given issues. In the proposed method, the parameter line data, load and generator data with its LB and UB are initialized.

$$X_{ij} = rand \times (UB_j - LB_j) + LB_j, i = 1, 2, \dots, N, j = 1, 2, \dots, Dim \quad (28)$$

where  $rand$  represents a random number,  $LB_j$  denotes  $j$ th lower bound and  $UB_j$  signifies  $j$ th the upper bound of the problem.

#### 3.5 Step 2: fitness function

The fitness function is considered important for finding the best optimal solution in optimization. The fitness value of

the proposed method is taken as voltage stability margin and remaining load power (not fulfil load power).

$$f = \max(VSM_{sys} + P_{remainingload}) \quad (29)$$

where  $VSM_{sys}$  is the overall system VSM,  $P_{remainingload}$  is the total remaining load and  $f$  is the fitness function.

### 3.6 Step 3: updation

Each solution modifies its placements in accordance with the optimal result produced by the AO's optimization techniques. It is offered to highlight the balance between the AO's search tactics (i.e. expanded exploration, narrowed exploration, expanded exploitation and narrowed exploitation). The general form of updating the solution is stated in Eq. (30).

$$X_M(t) = \frac{1}{N} \sum_{i=1}^N X_i(t), \forall j = 1, 2, \dots, Dim \quad (30)$$

where  $Dim$  indicates the dimensional area of issues and  $N$  represents the integer of the inhabitant area.

### 3.7 Step 4: termination

The process is repeated until the best value of the parameter is obtained, and the procedure ends when the best solution is found.

Figure 3 shows the proposed optimal load shedding approach provides a well perform at the island period. It shed the load based on the priority limit, and curtailment was done to remove the remaining load. During optimal shedding, the power flow was maintained and the voltage stability margin was kept within a limit. The performance evaluation of the proposed islanding detection and optimal shedding period was stated as follows.

## 4 Result and discussion

In this section, the intelligent controller-based islanding detection and optimal load shedding model is designed and observed in its performance. In the proposed work, one of the phases describes the analyses of 6 types of island detection or grid-connected mode of the IEEE 30-bus system model. The parameters of current and voltage are sensed by sensors. The parameters are given to an advanced neural network. RNN can check the proposed network whether it is island or normal. If an islanding condition is detected, then proceed the process of load scheduling or normal condition occurs power supply continues to the grid and fulfils the power requirement in consumers. MATLAB 2021a/Simulink on an Intel Core i5

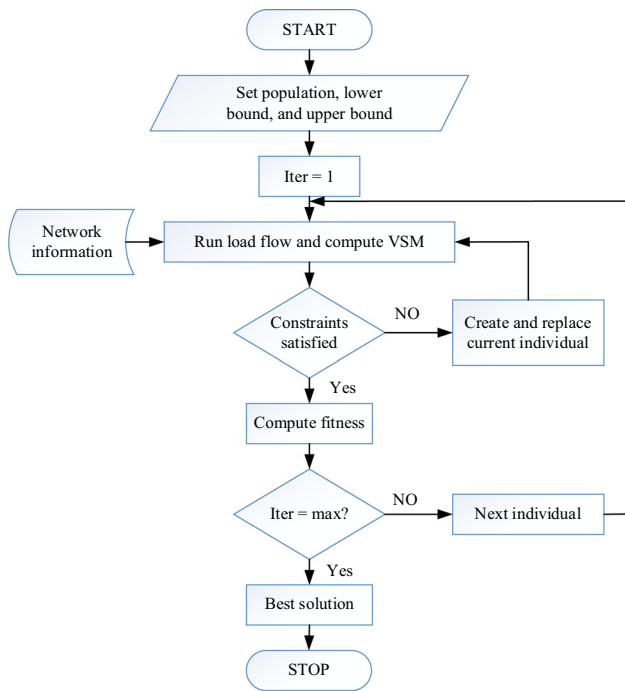


**Fig. 3** Proposed load shedding model flowchart

processor, Windows × 64-bit and 8 GB of RAM is used to execute and evaluate the optimal load shedding strategy. The G1 is first assumed to be a utility grid while designing the initial IEEE 30-bus architecture. An intelligent controller is designed to detect whether the system is normal or islanding. After detecting the islanding, the load is shed based on the generation at an individual period. During the shedding period, the voltage stability of all buses are maintained constantly. The proposed model's working process consists of two operations phases that are observed values are discussed in the following sections.

#### 4.1 Phase 1: island detection

The hybrid islanding detection method that is being presented purposely introduces an unstable condition into the system that only appears in islanding conditions and is a

**Table 2** Amount of samples for testing and training

Period	Number of samples
Testing	2800
Training	11,200

means to identify this instability when islanding occurs. Real-time dataset was created to make a detection controller which senses the PCC power and detects the condition of a system. The dataset creation was discussed as follows.

##### 4.1.1 Dataset creation

The IEEE 30-bus system consists of 6 generators, 21 load buses and 41 transmission lines. Generator G1 connected to the utility grid, G2, G3, G4, G5 and G6 are considered renewable energy resources and constant power DG. There are six types of short-circuit faults that can occur in a system, including double- and triple-line-to-ground faults, line-to-ground faults, load switching and capacitance switching to collect the power data from the generator buses, as shown in Table 1. It demonstrates 14,000 samples are collected from the designed model; in each condition, 2000 samples are labelled to train the detection controller. This dataset is given to the RNN input to train based on the trained value the intelligent mode detection controller detects the system condition. The training and testing data samples are shown in Table 2. It shows the 11,200 samples for training data and 2800 samples for testing data around the 14,000 samples.

The proposed model effectively predicts the system conditions like island mode or normal mode. Once the islanding is detected, move on to optimal priority-based load scheduling, or normal condition occurs continuity to the power supply to the consumer. This method is more effective as compared to existing methods. The proposed model simulation parameters and existing methods parameters are evaluated, which is given in Table 3.

Based on the above-mentioned ranges, the proposed detection controller was created to detect the exact stage of a

**Table 1** Data samples and labels for classifier

System Event	Type	Target	Sampling data
Without fault condition	Normal	1	2000
Double-line-to-ground fault	Line fault	2	2000
Line-to-ground fault		3	2000
Three-phase-to-ground fault		4	2000
Capacitor switching	Overvoltage fault	5	2000
Load switching		6	2000
Grid-disconnected mode	Islanding	7	2000

**Table 3** Simulation parameter of the detection model

Method	Parameter	Ranges
RNN	Mini batch size	2
	Hidden layer	10
	Maximum epochs	1
DNN	Learning	0.001
	Activation function	ReLU
	Optimizer	Adam
ANN	Hidden layer	6

system. During the normal condition, the waveform of each bus is constant because there is no more fault happened in the system. The waveforms of normal and islanding modes are observed and sketched in Figs. 4 and 5.

The experimental setup of a three-phase generator in normal conditions is shown in Fig. 4. Figure 4 illustrates the generator’s continuity of operations. Figure 4a demonstrates the generator 1 power flow analysis. Figure 4a clearly shows the continuous power flow in 0 to 0.32 W in generator 1. Figure 4b illustrates the generator 2 power flow analysis. Figure 4b clearly shows the continuous power flow from – 0.07 to 0.26 W. Figure 4c demonstrates the generator 3 power flow analysis. Figure 4c shows the continuous power flow

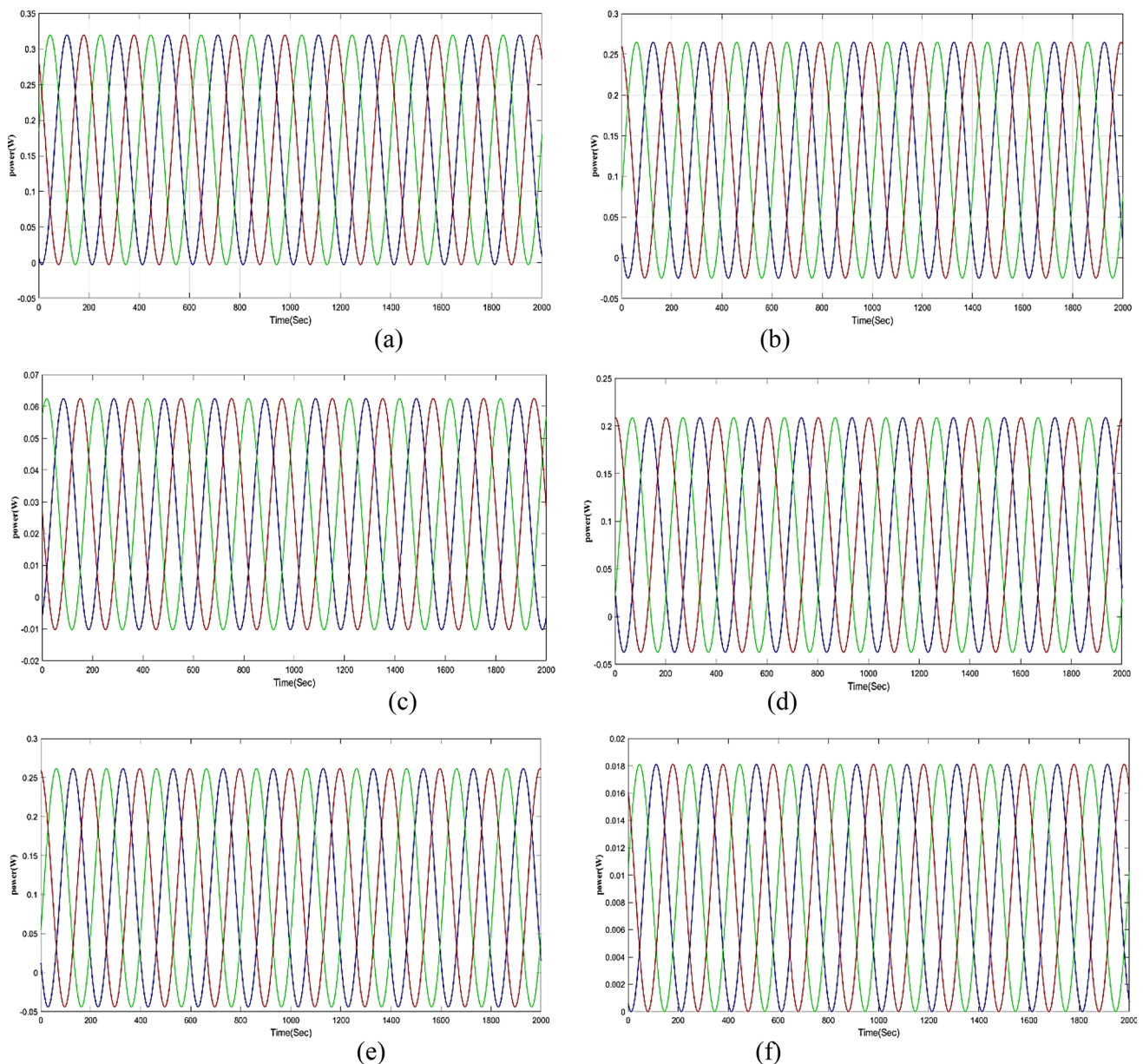


**Fig. 4** Analysis of power flow in normal condition: a G1, b G2, c G3, d G4, e G5, f G6

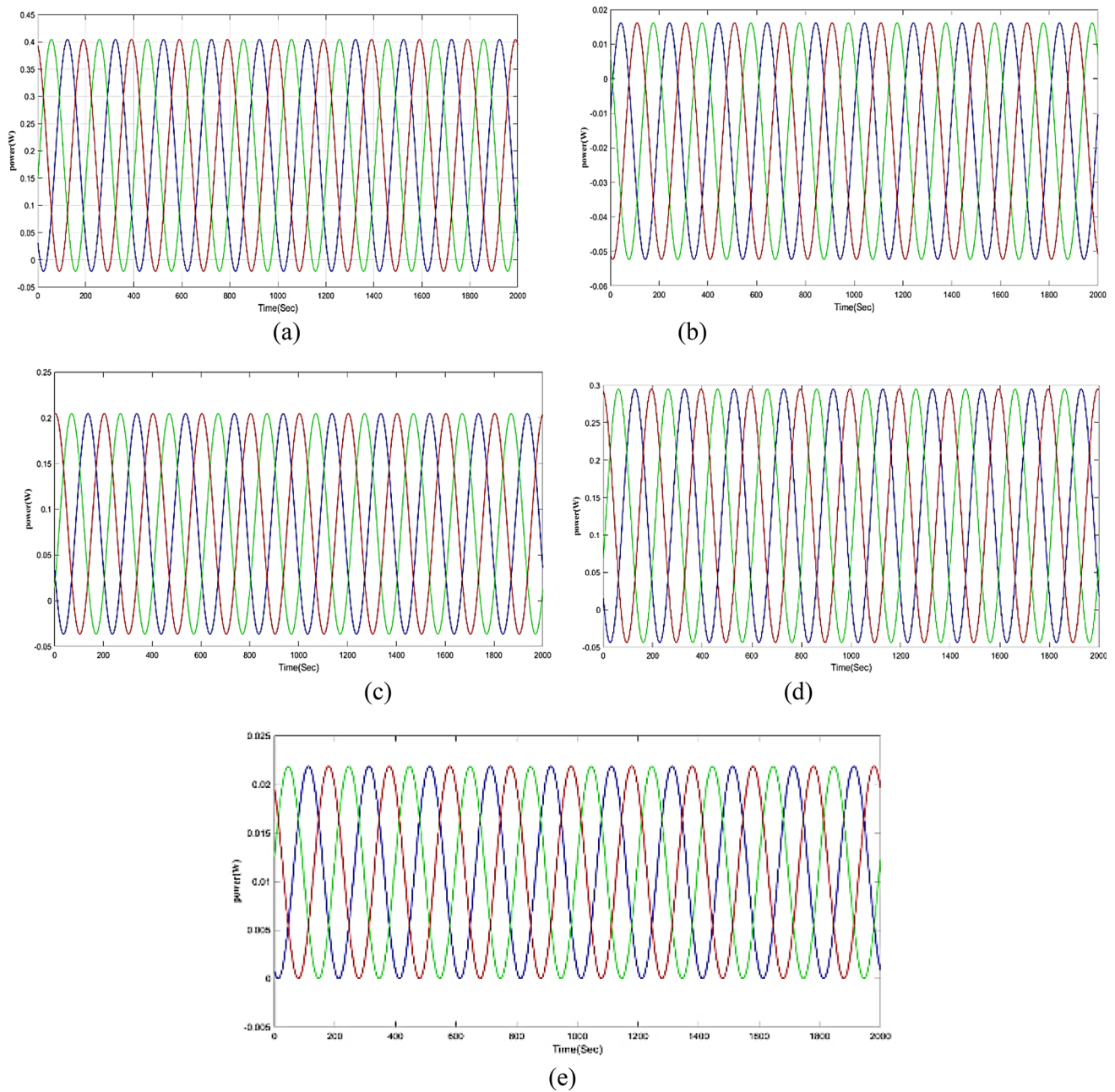


**Fig. 5** Analysis of power flow in normal condition: **a** G1, **b** G2, **c** G3, **d** G4, **e** G5

from  $-0.01$  to  $0.061$  W. Figure 4d demonstrates the generator 4 power flow analysis. Figure 4d shows the continuous power flow from  $-0.06$  to  $0.21$  W. Figure 4e illustrates the generator 5 power flow analysis. Figure 4e clearly shows the continuous power flow from  $-0.06$  to  $0.26$  W. Figure 4f demonstrates the generator 6 power flow analysis. Figure 4f shows the continuous power flow from  $0$  to  $0.018$  W.

**Island condition** In this mode, the grid is disconnected from the bus system due to a fault arise. During this period, the voltage of each bus collapsed, so the load power was varied,

thus causing severe causes at the end users. The waveform of five generator buses in this period is observed and plotted in Fig. 5.

Figure 5 depicts the experimental three-phase generator arrangement for an island location. The generator's operations are interrupted in the figure. Figure 5a demonstrates the generator 1 power flow analysis. Figure 5a clearly shows the power flow variation from  $-0.08$  to  $0.4$  W in generator 1. Figure 5b illustrates the generator 2 power flow analysis. Figure 5b shows the power flow variation from  $-0.051$  to  $0.016$  W. Figure 5(c) demonstrates the generator 3 power

**Fig. 6** Analysis of confusion matrix in the island state

1	69535			10	53	51	6
2		29151		49			11
3			8208	4			
4	60	13	10	18897			4
5	19				68850	24	57
6	64			1	43	4952	2
7		41	10	17	25		19844
	1	2	3	4	5	6	7

flow analysis. Figure 5c shows the power flow variation from  $-0.06$  to  $0.2$  W. Figure 5d demonstrates the generator 4 power flow analysis. Figure 5d shows the power flow variation from  $-0.06$  to  $0.29$  W. Figure 5e illustrates the generator 5 power flow analysis. Figure 5e shows the power flow variation from  $0$  to  $0.022$  W. The created controller analyses these power variations to detect the system's condition.

**Confusion matrix** A machine learning model's performance on a set of test data is summarized in a matrix called a confusion matrix. It is frequently used to gauge the effectiveness of categorical label prediction models, which seek to predict a categorical label for each input event. The matrix shows the quantity of true negatives (TN), true positives (TP), false negatives (FN) and false positives (FP) that the model on the test data produced.

Figure 6 shows the analysis of the confusion matrix in the island state. The created dataset was split into two groups for training and testing to detect the condition of bus system. As shown in Fig. 6, the actual class values for the first, second, third, fourth, fifth, sixth and seventh classes are 69,535, 29,151, 8208, 18,897, 68,850, 4952 and 19,844, respectively, and 574 samples are wrong predicted. This confusion matrix was used to evaluate the controller's performance and contrast it with some other recent approaches.

#### 4.1.2 Comparative analysis

The suggested model contrasts with other existing approaches to validate the performance. The existing approaches are considered as deep neural networks (DNN) and artificial neural networks (ANN). The comparison was held on the accuracy, F1 score, error, kappa, precision, specificity and sensitivity. Figures 7 and 8 demonstrate the comparison of suggested and traditional model performance.

The system that predicts a value with the least degree of error is said to be accurate. Figure 7a illustrates the accuracy of the suggested and current methods. The proposed method has a 99% accuracy rate compared to DNN 97% and ANN's 92%. The error value of the suggested and present methods are then compared. The degree of errors or issues in a system is known as its error level. The system operates worse when the error is high and better when the error is low. The comparison of errors between the suggested and present methods is shown in Fig. 7b. The suggested approach has a 1% error rate, compared to 3% for DNNs and 9% for ANNs. The value of the F1 score for the suggested and existing methodologies is then examined. The binary kinds of the system and the degree of dataset accuracy are revealed by a statistical analysis of the F1 score. Figure 7c compares the projected and actual F1 scores. The F1 score value for the proposed technique is 99%, DNN is 97%, and ANN is 69%. Figure 7d shows the kappa comparison between the proposed and existing techniques. The consistency of numerous variables at various rates is measured by kappa. The suggested model kappa value is 99%, DNN is 90%, and ANN is 68%.

The precision comparison between the suggested and present models is shown in Fig. 8a. Accurate measurement is sometimes defined as the number of positive events that can be reliably predicted. The accuracy of the proposed model is 99%, which is higher than the accuracy of other modern approaches like DNN and ANN, which have accuracy values of 97% and 69%, respectively. Figure 8b compares the sensitivity of suggested and existing techniques. The proportion between what is actually positive and how exactly a positive is acknowledged. The proposed method's sensitivity is 99%, DNN's is 97%, and ANN's is 70%. The level of specificity of the suggested and existing procedures is compared in Fig. 8c. The specificity of a model refers to how accurately it can predict the actual negatives for each conceivable kind. Compared to two existing techniques, DNN and ANN,

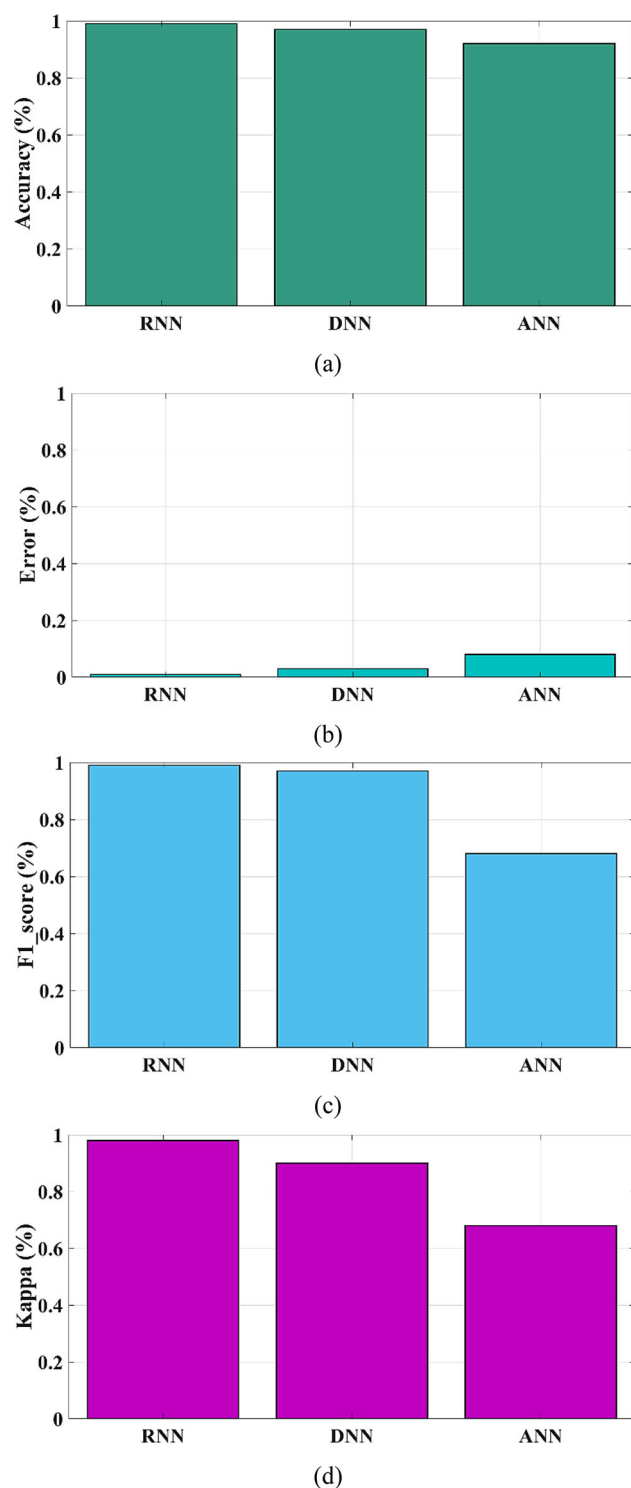


**Fig. 7** Analysis of suggested and present approaches: **a** accuracy, **b** error, **c** F1 score, **d** kappa

with equal specificity values of 99% and 98%, the proposed method's specificity value was 99%.

Then the proposed model performance metrics are compared to some other current approaches like SVM,

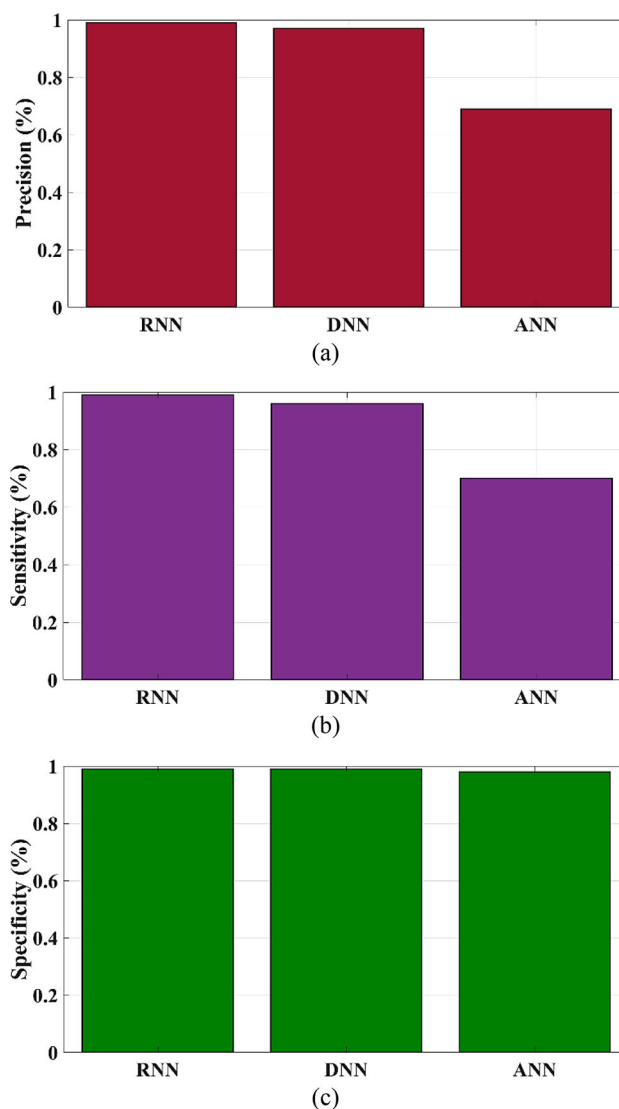


**Fig. 8** Analysis of suggested and present approaches: **a** precision, **b** sensitivity, **c** specificity

multi-feature-based SVM, pure backpropagation (BP) and improved LSTM. The comparison was held on the accuracy, precision and F1 score as shown in Table 4.

A comparison of the suggested method's performance with the results of the currently used methods is given in Table 4 [36]. The capacity of a model to predict a value with the least degree of error is measured by its accuracy. The proposed approach has an accuracy rate of 99%, which is higher than SVM, which has 65%, multi-feature + SVM has 63%, pure BP has 93%, and improved LSTM has 98%. Precision is a term used to describe precise measurement and is defined as the total number of real actions that may be accurately predicted. Precision is a term used to describe exact measurement and is defined as the total number of positive events that may be accurately predicted.

**Table 4** Comparative analysis of suggested and present approaches

Method	Accuracy (%)	Precision (%)	F1 score (%)
SVM	65	2	15
Multi-feature + SVM	63	2	17
Pure BP	93	96	85
Improved LSTM	98	1	96
Proposed	99	99	99

In comparison with other current approaches, such as SVM, multi-feature + SVM and pure BP, improved LSTM with corresponding precision values of 2%, 2%, 96% and 1%, the suggested method's precision value was discovered to be 99%. An analysis of the F1 score's statistical data exposes the binary kinds of the system and the degree of dataset accuracy. Table 4 displays a comparison of the planned and current F1 scores. The F1 score value for the proposed technique is 99%, SVM is 15%, multi-feature + SVM is 17%, pure BP is 85%, and improved LSTM is 69%. Compared to existing methods, the proposed method effectively predicts the island state.

## 4.2 Analysis of non-detection zone and detection time

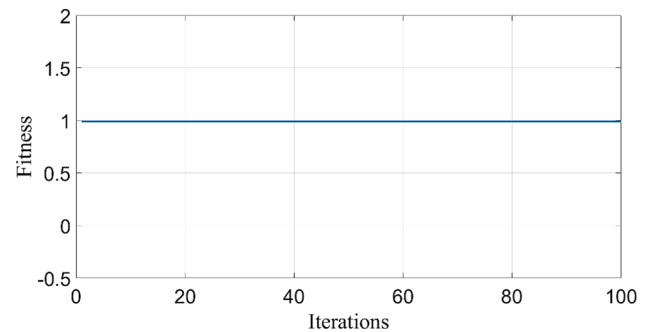
This section of the investigation further assesses the suggested RNN-based algorithm's effectiveness for each unique scenario involving generated power from DG and distribution network voltage range ( $U_N$ ). The voltage and generated power are restricted to the lowest and highest permit levels in the generated power and the voltage in the distribution network. For voltage levels ranging from  $-10\% U_N$  to  $+10\% U_N$  and 0% to 110% installed for generated power, the step is specified as 1% and 5%, respectively. The nominal distribution network voltage ( $U_n$ ) and the total installed capacity of DG correspond to these values. For those, a total of 17 events divided into three groups are simulated. The categories that follow are,

1. Islanding state with the least amount of power imbalance
2. Grid-connected mode with minimum power exchange
3. Grid-connected mode with capacitor switching at minimum power exchange

The above-mentioned cases are utilize to analyse the system's non-detection zone performance. The performance metrics of proposed RNN model is presented in Table 5. It shows the proposed model provide an effective performance at this non-detection zone period.

**Table 5** Performance metrics of proposed model at non-detection zone

Metrics	Values
Accuracy	0.98
Precision	0.99
Sensitivity	0.99
Specificity	0.97
FPR	0.14
F1 score	0.99

**Fig. 9** Convergence graph of AO

If the island is detected, the load must be scheduled to manage the power flows with low cost. The load scheduling model is discussed in the following section.

## 4.3 Phase 2: load shedding

When an island condition is present, the loads become unbalanced. One of the best ways to reduce load unbalancing difficulties is to use load shedding. The voltage stability of all buses remains constant during the shedding time. The following sections discuss the observed values from the proposed phase 2 model working process.

### 4.3.1 Convergence graph of AO

Figure 9 illustrates the proposed model convergence graph. In this graph, fitness functions consider as voltage stability margin. The voltage stability margin on a tie line is the difference between the limit and the actual power transmission. To maintain voltage stability constant to help to prevent system blackouts. The AO curve constantly maintains in fitness function 1 in 1st iteration.

The most promising demand-side management strategy is load shedding, in which consumers move demand from peak to off-peak times to reduce grid power peak and electricity bill costs. When an island condition exists, the loads become unbalanced. One of the greatest ways to reduce load

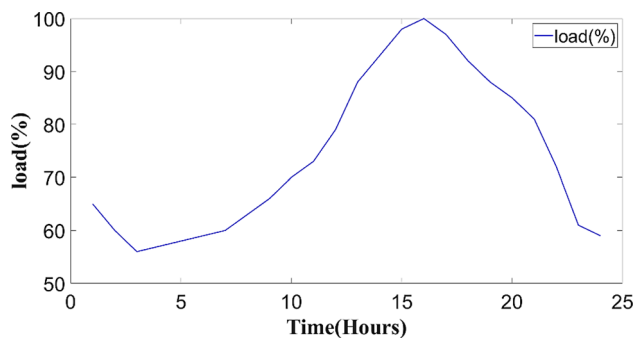


Fig. 10 Individual load profile analysis per day

unbalancing difficulties is to use priority-based load shedding. Making a load schedule might help you estimate how much power is needed for an installation. One of the most important parts of load scheduling is load control and management.

The study on the optimum load shedding strategy is clearly illustrated in Fig. 10. According to the type and time of day, different DG power injections are made into the four DG units, which are thought of in this study as constant power sources. The several categories of DGs and their maximum active power ratings are displayed in Table 5. As part of the load shedding study, each individual load profile is displayed in Fig. 10. According to a base case bus power value derived from the original IEEE 30-bus technology, 100% of the load is active at 16.00 period.

A detailed summary of the proposed load shedding plan’s performance in grid-disconnected mode (island mode) is illustrated in Fig. 11. Figure 11a illustrates how the amount of load left over after optimization is comparable to the quantity of power generated throughout the hourly operation. This result demonstrates that the recommended optimal load shedding technique based on the AO can determine the proper amount of load to shed without removing the excessive load from the system. After optimization, the difference between power generation and load demand constitutes the system’s power loss, as shown in Fig. 11a. While DG1 and DG3 provide the system with support from their PV generators, there is barely any power loss.

On the other hand, when PV DGs are not in use, power loss is greater in the evening and early morning. Figure 11b illustrates that the suggested load shedding technique results in a load profile that is higher than the load priority limitations. The proposed AO-based load shedding technique, therefore, seems to be able to meet the load priority limit requirement.

According to the type and time of day, different DG power injections are performed into the five DG units, regarded as continuous power sources in this study. Table 5 shows the different types of DGs and their maximum active power

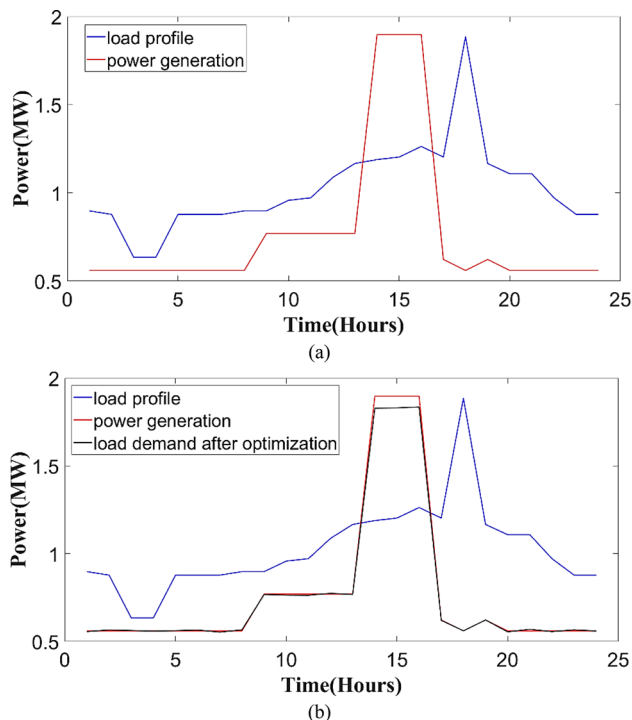


Fig. 11 Analysis of optimal load shedding at island condition

Table 6 DG maximum power rating

Generator	Type	Maximum power rating (MW)
1	PV1	0.265
2	Wind	0.0625
3	PV2	0.21
4	DG1	0.26
5	DG2	0.3

ratings. The PV1 rating is 0.265 MW, the wind turbine rating is 0.0625 MW, the PV2 rating is 0.21 MW, the DG1 rating is 0.26 MW and DG2 rating is 0.3 MW. During normal conditions, the power sources are delivered maximum as mentioned in Table 5; in island condition, the power of each bus is reduced to the maximum power. The required parameter settings for the optimization strategies employed in this investigation are listed in Table 6.

The statistical results for fitness value and VSM are provided in the correct sequence in Table 7. The best load shedding results for power islands were achieved by AO with a stable fitness. According to Table 7, the proposed model’s fitness values are 2.02, and a 37% VSM reduction was used for the load curtailment. This discovery shows that the suggested AO-based optimal load shedding strategy can select the ideal load to shed without considerably decreasing the system load.



**Table 7** AO parameter ranges

Parameter	AO
$\beta$	1.5
A	0.1
$\Delta$	0.1
$\Omega$	0.005

Then the proposed optimal shedding scheme was validated under various generating conditions. The generation is reduced to 320 MW and analysed the shedding performance. The proposed model provides 16.8 MW shedding and 8.5 MW losses during this period. Same as the generation was changed to 300 MW, 315 MW and 290 MW. In these instances, the load shed is 36.2 MW, 21.6 MW and 46 MW, respectively. Table 8 shows the load shed under various generation conditions.

The proposed optimal shedding model provides a better outcome to secure the bus system. It offers low losses and satisfies the load as per the generation. Once the island is detected, the proposed shedding scheme sheds the load based on the generation. Then proposed RNN model detection zone is compared to some other traditional approaches like hybrid with fuzzy and hybrid technique. The non-detection zone was a loading condition for which an islanding detection method would fail to operate in a timely manner (Table 9).

The comparative analysis demonstrates the proposed model detects the fault at a few milliseconds (ms) than the traditional approaches, because the existing models are inaccurate data and inputs, and imprecise nature of logic. As compared to this approaches, the proposed model detect all fault without fails. The proposed model detects the fault/islanding condition to shed the load based on the priority to overcome the non-detection zone issues using RNN controller and AO (Table 10).

## 5 Conclusion

The system was secured during the island time using a unique islanding detection and load shedding approach. When there is no longer access to the external electrical grid, a DG keeps an area powered, a circumstance known as islanding. In the

**Table 9** Load shed under various generation conditions

Power generation (MW)	Amount of load shed (MW)	Losses (MW)
320	16.8	8.5
300	36.2	7.8
315	21.6	8.2
290	46	7.6

proposed work, an IEEE 30-bus system with parameters for voltage and current sensed by sensors is designed. Seven types of faults were applied individually in the system to make real-time data and used to train the intelligent detection controller, which can distinguish between the island and normal mode. Move on load scheduling if island mode is detected; else, keep supplying power to the grid to meet consumer demand. The optimum load shedding method involves analysing the generation and distributing the load according to priority. The multi-objective optimization problem was solved using the AO by maximizing the remaining load bus powers and retaining the VSM in all buses. Therefore, the islanding detection method can be combined with the best load shedding technique in a real power distribution system with DGs. The bus, load and generation data were initialized to shed the load with its priority range. The proposed method has been tested in both islanding (grid-disconnected) and grid-connected modes. The suggested approach enables effective energy flow control to lower costs for both modes. The suggested method for detecting islanding is equally successful as more modern methods like ANN and DNN. The proposed model offers 99% accuracy at detection performance and also offers 37% load curtailment with 0.988 VSM. The proposed model was well fit for all atmospheric conditions and in any system. The impacts that face in proposed model was that it cannot process very long sequences if using tanh or ReLU as an activation function. So in future work, an advance island detection approach will be designed to identify various fault conditions and shedding the load at all fault period using intelligent shedding scheme at huge sequence data.

**Table 8** Performance of AO in terms of fitness and VSM at 1 h

Condition no	Fitness		VSM		Load curtailment (%)
	Before optimization	After optimization	Before optimization	After optimization	
7	–	2.02	1.0335	0.9888	37%

**Table 10** Comparison of island detection time (ms) [37]

Faults	Proposed RNN	Hybrid with fuzzy	Hybrid technique
Generation < load	0.0053	0.0092	0.0121
Generation = load	0.0234	0.0652	–
Generation > load	0.0086	–	0.0171
Single-phase fault	0.00657	–	0.0082
Double-phase fault	0.0053	–	0.0077

**Author contributions** The corresponding author claims the major contribution of the paper including formulation, analysis and editing. The co-author provides guidance to verify the analysis result and manuscript editing.

**Funding** The authors declare that no funds, grants or other support were received during the preparation of this manuscript.

## Declarations

**Conflict of interest** The authors declared that they have no conflicts of interest to this work. We declare that we do not have any commercial or associative interest that represents a conflict of interest in connection with the work submitted. This article is a completely original work of its authors; it has not been published before and will not be sent to other publications until the journal's editorial board decides not to accept it for publication.

## References

- Ghulomzoda A, Safaraliev M, Matrenin P, Beryozkina S, Zicmane I, Gubin P, Gulyamov K, Saidov N (2021) A novel approach of synchronization of microgrid with a power system of limited capacity. *Sustainability* 13(24):13975
- Raja K, Patan MK, Ahmed MA, Ganeshan P (2022) Water evaporation algorithm optimized cascade controller for frequency regulation of integrated microgrid. *J Intell Fuzzy Syst* 43(5):5535–5549
- Sathish T, Subramanian DB, Muthukumar K, Karthick S (2020) Design and simulation of wind turbine on rail coach for power generation. *Mater Today Proc* 33:2535–2539
- Ashwin KV, Kosuru VSR, Sridhar S, Rajesh P (2023) A passive islanding detection technique based on susceptible power indices with zero non-detection zone using a hybrid technique. *Int J Intell Syst Appl Eng* 11(2):635–647
- Kumar SA, Subathra MS, Kumar NM, Malvoni M, Sairamya NJ, George ST, Suviseshamuthu ES, Chopra SS (2020) A novel islanding detection technique for a resilient photovoltaic-based distributed power generation system using a tunable-q wavelet transform and an artificial neural network. *Energies* 13(16):4238
- Özcanlı AK, Baysal M (2022) A novel Multi-LSTM based deep learning method for islanding detection in the microgrid. *Electric Power Syst Research* 202:107574
- Pouryekta A, Ramachandaramurthy VK, Mithulananthan N, Arulampalam A (2017) Islanding detection and enhancement of microgrid performance. *IEEE Syst J* 12(4):3131–3141
- Wu H, Zhang Y, Chen R, Ding K, Gong D, Dai S, Wei X, Yu Y, Yao H (2019) A microgrid system with multiple island detection strategies. In 2019 IEEE PES Asia-pacific power and energy engineering conference (APPEEC) (pp. 1–4). IEEE.
- Xia Y, Yu F, Xiong X, Huang Q, Zhou Q (2022) A novel microgrid islanding detection algorithm based on a multi-feature improved LSTM. *Energies* 15(8):2810
- Radhakrishnan RM, Sankar A, Rajan S (2020) Synchrophasor based islanding detection for microgrids using moving window principal component analysis and extended mathematical morphology. *IET Renew Power Gener* 14(12):2089–2099
- Shahid MU, Alquthami T, Siddique A, Munir HM, Abbas S, Abbas Z (2021) RES based islanded DC microgrid with enhanced electrical network islanding detection. *Energies* 14(24):8432
- Shafique N, Raza S, Bibi S, Farhan M, Riaz M (2022) A simplified passive islanding detection technique based on susceptible power indice with zero NDZ. *Ain Shams Eng J* 13(4):101637
- Arif A, Imran K, Cui Q, Weng Y (2021) Islanding detection for inverter-based distributed generation using unsupervised anomaly detection. *IEEE Access* 9:90947–90963
- Liu J, Zhang Y, Meng K, Dong ZY, Xu Y, Han S (2022) Real-time emergency load shedding for power system transient stability control: a risk-averse deep learning method. *Appl Energy* 307:118221
- Elyasichamazkoti F, Teimourzadeh S, Aminifar F (2022) Optimal distribution of power grid under-frequency load shedding with security considerations. *IEEE Trans Power Syst* 37(5):4110–4112
- Hou K, Tang P, Liu Z, Jia H, Yuan K, Sun C, Song Y (2022) A fast optimal load shedding method for power system reliability assessment based on shadow price theory. *Energy Rep* 8:352–360
- Arigela SH, Krishnan TS, Krishnakumar SK, Mohanraj A, Mahajan MR (2022) A study on the functionality of PID and fuzzy logic controllers for Quadratic Boost Converter (Qbc). In: 2022 international conference on power, energy, control and transmission systems (ICPECTS). IEEE, pp 1–7
- Alam SM, Ali MH (2020) A new subtractive clustering based ANFIS system for residential load forecasting. In 2020 IEEE power & energy society innovative smart grid technologies conference (ISGT) (pp. 1–5). IEEE.
- Malik S, Lee K, Kim D (2020) Optimal control based on scheduling for comfortable smart home environment. *IEEE Access* 8:218245–218256
- Kalakova A, Nunna HK, Jamwal PK, Doolla S (2021) A novel genetic algorithm based dynamic economic dispatch with short-term load forecasting. *IEEE Trans Ind Appl* 57(3):2972–2982
- Elshrief YA, Helmi DH, Abd-Elhaleem S, Abozalam BA, Asham AD (2021) Fast and accurate islanding detection technique for microgrid connected to photovoltaic system. *J Radiat Res Appl Sci* 14(1):210–221
- Abdelsalam AA, Salem AA, Oda ES, Eldesouky AA (2020) Islanding detection of microgrid incorporating inverter based DGs using long short-term memory network. *IEEE Access* 8:106471–106486
- Karimi M, Farshad M, Hong Q, Laaksonen H, Kauhaniemi K (2020) An islanding detection technique for inverter-based distributed generation in microgrids. *Energies* 14(1):130
- Dutta S, Olla S, Sadhu PK (2021) A secured, reliable and accurate unplanned island detection method in a renewable energy based microgrid. *Eng Sci Technol, Int J* 24(5):1102–1115

25. Ali W, Ulasyar A, Mehmood MU, Khattak A, Imran K, Zad HS, Nisar S (2021) Hierarchical control of microgrid using IoT and machine learning based islanding detection. *IEEE Access* 9:103019–103031
26. Ramachandradurai S, Krishnan N, Prabakaran N (2022) Unintentional passive islanding detection and prevention method with reduced non-detection zones. *Energies* 15(9):3038
27. Alhelou HH (2019) Under frequency load shedding techniques for future smart power systems. In *Handbook of research on smart power system operation and control* (pp. 188–202). IGI Global.
28. Rauf S, Kalair AR, Khan N (2020) Variable load demand scheme for hybrid AC/DC nanogrid. *Int J Photoenergy* 2020:1–40
29. Hassan YF, Rashid YG, Tuaimah FM (2019) Demand priority in a power system with wind power contribution load shedding scheme based. *J Eng* 25(11):92–110
30. Mogaka LO, Nyakoe GN, Saulo MJ (2020) Power prioritization and load shedding in an island with RESs using ABC algorithm. *J Eng* 2020:1
31. Awad H, Hafez A (2022) Optimal operation of under-frequency load shedding relays by hybrid optimization of particle swarm and bacterial foraging algorithms. *Alex Eng J* 61(1):763–774
32. Sarasúa JI, Martínez-Lucas G, Pérez-Díaz JI, Fernández-Muñoz D (2021) Alternative operating modes to reduce the load shedding in the power system of El Hierro Island. *Int J Electr Power Energy Syst* 128:106755
33. Xu J, Xie B, Liao S, Yuan Z, Ke D, Sun Y, Peng X (2021) Load shedding and restoration for intentional island with renewable distributed generation. *J Modern Power Syst Clean Energy* 9(3):612–624
34. Matic-Cuka B, Kezunovic M (2014) Islanding detection for inverter-based distributed generation using support vector machine method. *IEEE Transact Smart Grid* 5(6):2676–2686
35. Pawar P, Sampath S, Ghosh T, Vittal KP (2018) Load scheduling algorithm design for smart home energy management system. In: *2018 IEEE 7th international conference on power and energy (PECon)* (pp. 304–309). IEEE.
36. Melhem FY, Grunder O, Hammoudan Z, Moubayed N (2018) Energy management in electrical smart grid environment using robust optimization algorithm. *IEEE Trans Ind Appl* 54(3):2714–2726
37. Elshrief YA, Asham AD, Bouallegue B, Ahmed A, Helmi DH, Abozalam BA, Abd-Elhaleem S (2022) An innovative hybrid method for islanding detection using fuzzy classifier for different circumstances including NDZ. *J Radiat Res Appl Sci* 15(2):129–142

**Publisher's Note** Springer Nature remains neutral with regard to jurisdictional claims in published maps and institutional affiliations.

Springer Nature or its licensor (e.g. a society or other partner) holds exclusive rights to this article under a publishing agreement with the author(s) or other rightsholder(s); author self-archiving of the accepted manuscript version of this article is solely governed by the terms of such publishing agreement and applicable law.